Chapter 11. Juan de Fuca Strait

Physiography

Juan de Fuca Strait is a long, narrow submarine valley that originates along a depression between the resistant lava flows and metamorphic rocks of southern Vancouver Island and the Olympic Mountains (Fig. 11.1). Over the last 1–2 million yr, the Strait has undergone excavation on at least four separate occasions, as continental ice sheets moved seaward during periods of worldwide cooling.

East of the line between Jordan River and Pillar Point, the region is characterized by a gently sloping U-shaped, cross-channel profile linked to recent glacial processes. A large terminal moraine, the Victoria–Green Point sill, marks the furthest point of advance of an ancient ice sheet that once existed in the Strait. Westward of this area to the Pacific entrance off Cape Flattery, the Strait takes on a V-shaped profile that resembles a mature river valley. Further seaward, the channel turns sharply to the southwest where it becomes irregular and is cut with deep incisions such as the Juan de Fuca Canyon.

From its entrance to about 100 km (55 nm) eastward, the Strait is approximately 22–28 km wide (12–15 nm), but narrows to 18 km (10 nm) between Race Rocks and Angeles Point. It then widens again to around 40 km (21 nm) for the next 56 km (30 nm) to the eastern boundary near Whidbey Island. The depth of the Strait decreases gradually inland from around 250 m at mid- channel near its entrance to about 180 m at a distance of 70 km east of Cape Flattery. This eastward shoaling continues to the cross-channel sill that cuts across the Strait to the south of Victoria. Over the sill, depths are relatively shallow at only 55 m. To the east of this submarine ridge, the Strait contains several shallow banks through which the deepest channels lead into Haro Strait. The lesser channels lead into Rosario Strait, Admiralty Inlet, and Deception Passage. For the most part, depths within Juan de Fuca Strait are appreciably less than those in the Strait of Georgia.

The coastline of the Strait is relatively uniform with a low rocky shoreline abutted against cliffs to 20 m high. Centuries of wave action have turned much of the shore into rocky intertidal platforms that are often engulfed in kelp in summer. Though sandy sediments are scarce due to the weather-resistant nature of the rocks, numerous small beaches have developed which, in the eastern portion, consist mainly of pebble–cobble material with logs at the head of the beaches. In the western section there are many small pocket beaches of coarse sediments and a few narrow, sand beaches. Port San Juan near the Pacific entrance is the only major fiordlike opening along the northern shoreline and provides the largest freshwater source, the San Juan River, that flows directly into the Strait. There are also constricted openings into Sooke Inlet and Sequim Bay at the eastern end of the Strait, and a relatively large indentation into Port Discovery. (See Chapter 2 for other coastal features.)

Temperature and Salinity Distributions

With the exception of a few protected bays and partially enclosed regions like Sooke Basin, water temperatures throughout the Juan de Fuca Strait system remain uncomfortably cold year round.

In part, the water of the Strait is kept cool by direct exposure to the Pacific Ocean, which, despite exaggerated tales of a warm "Japan Current" flowing toward the coast,

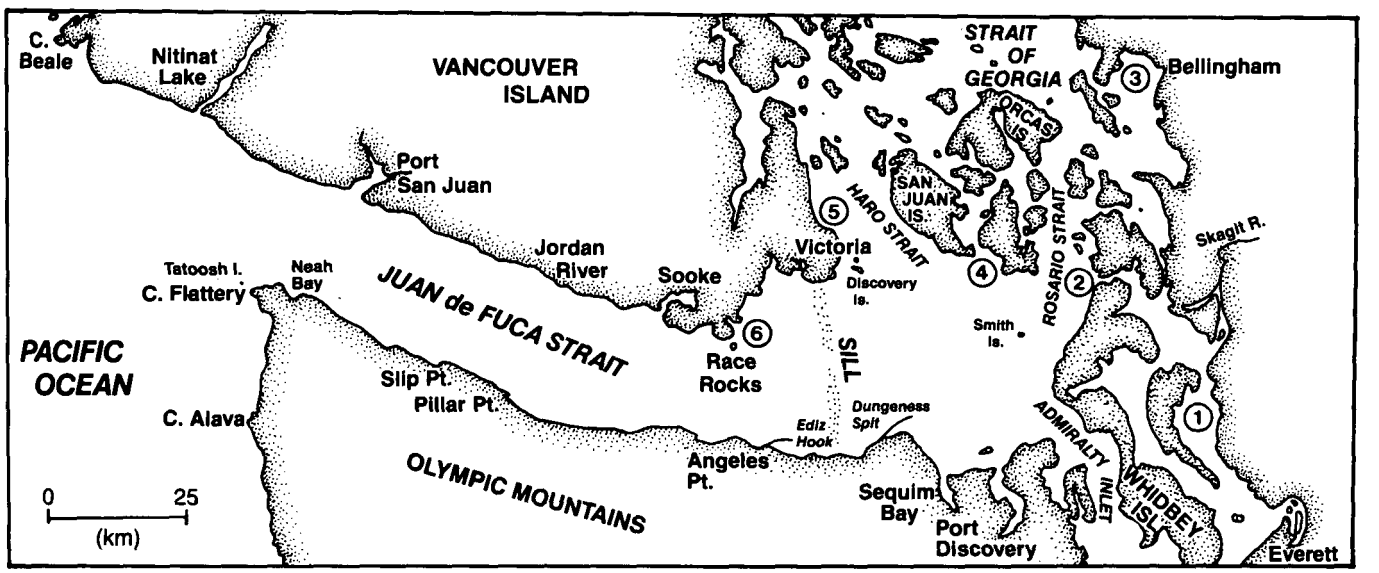

FIG. 11.1. Map of Juan de Fuca Strait and adjoining waters (1) Port Susan, (2) Deception Passage, (3) Bellingham Bay, (4) Middle Channel, (5) Cordova Bay, and (6) Pedder Bay.

coast, usually never warms above 12°C off Vancouver Island below depths of 10 m, even during the warmest summer months. But more importantly, the strong tidal streams through the eastern passes that adjoin the Strait constantly mix the water from top to bottom and make it nearly impossible for the surface layer to retain any appreciable amount of solar heat.

During winter, water temperatures near the surface generally decrease from relatively high values of 8–10°C near the Pacific entrance to comparatively low values of about 8°C in the eastern portion of the Strait (Fig. 11.2a). There is a corresponding reduction in water temperature with depth, though this rarely amounts to more than a few degrees. Nevertheless, it is in winter that near bottom temperatures are warmest in the western half of the Strait. East of the sill, between Victoria and Port Angeles, the water is invariably of uniform temperature from top to bottom because of intense tidal mixing in Haro Strait, Rosario Strait, and Admiralty Inlet.

About March, colder ocean water with temperatures around 6–7°C begins to penetrate up-channel along the bottom of Juan de Fuca Strait, but surface temperatures continue to remain slightly below 10°C (Fig. 11.2b). There is no appreciable change in the latter until the beginning of the spring freshet in the Strait of Georgia, when large volumes of fresh water commence to discharge from the Fraser River. Most of this water, which may warm to over 20°C in the near surface layer of the Strait of Georgia, works its way southward into the eastern basin of Juan de Fuca Strait. Although it has been tidally mixed with colder water enroute, it increases the total heat content of the water in Juan de Fuca Strait and raises average temperatures throughout its entire depth. With local solar heating, patches of surface water in the Strait can attain temperatures of 12–14°C by mid-August but bottom values continue to be cold (Fig. 11.2c). By September, surface water temperatures in the Strait of Georgia have diminished sharply and, in combination with the colder ocean water, enhanced wind activity, and substantially reduced solar radiation, cause surface temperatures along Juan de Fuca Strait to decrease to their eventual winter values of 8–10°C. In contrast, bottom waters begin to increase in temperature as warmer water slowly makes its way inland from the Pacific Ocean. By Christmas, temperatures are nearly uniform again throughout the entire channel.

Salinity of the water from the northern end of Haro Strait to the seaward end of Juan de Fuca Strait generally increases from top to bottom and from east to west (Fig. 11.3a). In simplest terms, the salt distribution can be likened to a "wedge" of saline water that has penetrated up-channel from the Pacific Ocean, but whose furthest point of advance is arrested by the partial barriers created by the series of sills to the east. Under favorable conditions, this "salt wedge" penetrates northward to the Strait of Georgia, where its identity is lost through tidal mixing in the vicinity of Boundary Passage.

In winter, salinities of the surface waters are commonly around 30–31‰, and those of the bottom water near the Strait entrance are relatively high at 33.5‰ (Fig. 11.3a, b). Rainfall and local river runoff can create shallow pools of low-salinity water at the surface at this time, but these are soon dispersed by winds and tides. With the advent of the spring runoff from the Fraser River, salinities in the upper layer can drop to around 26–28‰ in Haro Strait and to 28–30‰ in the eastern portion of Juan de Fuca Strait, as brackish water flows seaward from the Strait of Georgia (Fig. 11.3c). Coincident with this, there can be a slight increase in salinity near the open coast when upwelling (Chapter 5) associated with northwest winds brings cold, salty water onto the continental shelf. Thus, surface salinities in the vicinity of the entrance to Juan de Fuca Strait are generally greatest in summer and least in winter; to a lesser degree this is also true of the deeper water (compare Fig. 11.3a and 11.3c).

Clearly, temperature and salinity distributions in Juan de Fuca Strait are strongly influenced by oceanic conditions, river runoff, and tidal processes. However, seasonal variations in these water properties are quite small and for the most part would go unnoticed by the casual observer.

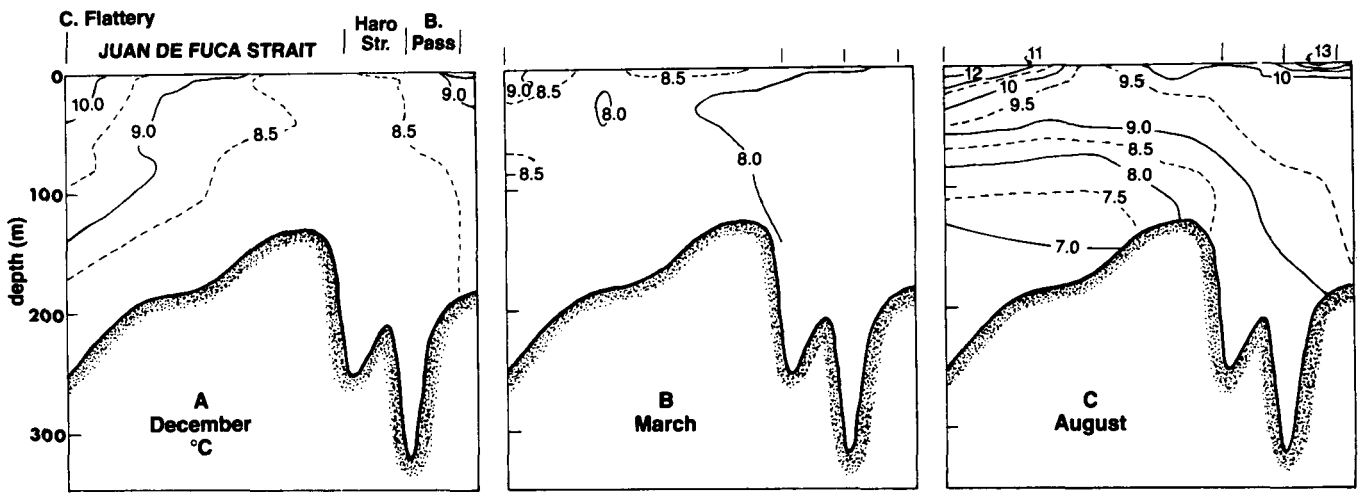

FIG. 11.2. Temperature distribution (°C) from Cape Flattery to Haro Strait, mid-channel; (A) December 1967, (B) March 1968, and (C) August 1968. (Adapted from Crean and Ages 1971)

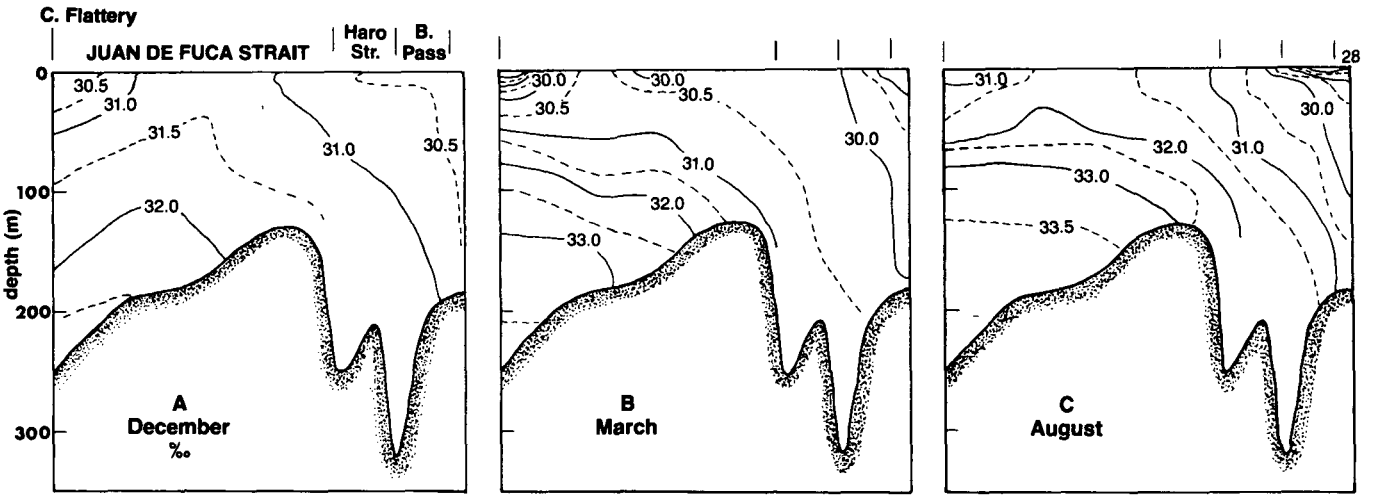

FIG. 11.3. Salinity distribution (‰) from Cape Flattery to Haro Strait, mid-channel; (A) December 1967, (B) March 1968, and (C) August 1968. (Adapted from Crean and Ages 1971)

Wind Patterns

Prevailing oceanic winds off the outer British Columbia–Washington coast are from the southwest in winter and the northwest in summer. Within Juan de Fuca Strait, where the flow of air is strongly influenced by the adjoining mountainous terrain, the corresponding wind directions are easterly in winter and westerly in summer (Fig. 11.4). In most cases, there is an overall increase in wind speed from east to west along the channel, and comparatively weak and variable winds prevail over the eastern sector. On a seasonal basis, winds greater than 15 m/s (30 kn) occur during 10–15 days per month in winter, compared to only 1–2 days per month in summer.

Easterly winds over Juan de Fuca Strait in winter (October–March) are, for the most part, associated with cyclonic oceanic winds of the Aleutian Low (see Fig. 2.14). Because of the funneling effect of the topography, these easterly winds undergo a seaward acceleration along the Strait; at Tatoosh Island off Cape Flattery for example, 38% have speeds in excess of 8.5 m/s (17 kn) whereas at Port Angeles at the eastern end of the Strait only about 5% exceed this value (Fig. 11.5). Average winter winds over the western portion of the channel are 10 m/s (20 kn). Observations taken off the coast from ships indicate that seaward-blowing winds along the Strait generally shift to southeasterlies a few kilometres off Cape Flattery, to suggest a combined influence of the southwesterly oceanic wind pattern and the locally funneled easterly winds of the channel.

Frontal systems that accompany eastward traveling cyclonic disturbances, formed in the central Pacific between the Aleutian Low and the Pacific High, often lead to rapid changes in the wind within the outer reaches of the Strait. As the low moves north of the channel, the prevailing south to southwesterly flow of coastal air backs to west-northwest as the cold front passes. Under certain conditions, moreover, predominant winter winds can be westerly along the Strait rather than easterly. This happened during the winter of 1976, accompanied by southwesterly winds along the outer coast of Washington. Such anomalous wind conditions are presumably linked in part to a greater than normal eastward shift of the midwinter Aleutian Low in the Gulf of Alaska, which in turn intensifies the westerly component of the onshore flow that favors westerly winds along the Strait.

Because of divergence in the airflow in the eastern portion of the Strait, winds to the east of Port Angeles blow predominantly from the west and southwest which, in winter, conforms to the general counterclockwise wind pattern that sets up over the southern half of the Strait of Georgia (see Fig. 10.5). During these months, winds at Victoria are mostly from the north and northeast, although easterlies and southeasterlies occur with regularity (about 20–30% of the time). As a consequence of the paths taken by individual fronts, moreover, winds from the west and southwest also occur. The frequency of such winds is high in October and March (about 30–40%) and low in December and January (about 18%). On the average, these winds are somewhat stronger than those from other quadrants.

Wind patterns in the eastern sector of the Strait are further complicated by the inertia of local air flow. Prior to the passage of a storm with southwesterly winds along the coast, the air is channeled through Puget Sound and around the Olympic Mountains (Fig. 11.6). In the lee of the mountains the winds overshoot, and leave an area of calm airs in the vicinity of Port Angeles. As the storm moves to the northeast, winds in the Strait turn to westerlies and the area of calm airs shifts southward to Puget Sound.

Wind patterns in spring are not appreciably different from winter except for a decrease in frequency of storms and front-related wind shifts.

In summer (June–September), when the air flow is dominated by the North Pacific High off California, winds along the coast are mainly from the northwest. These are redirected to inward-blowing westerlies within the Strait by the steering action of the mountains where

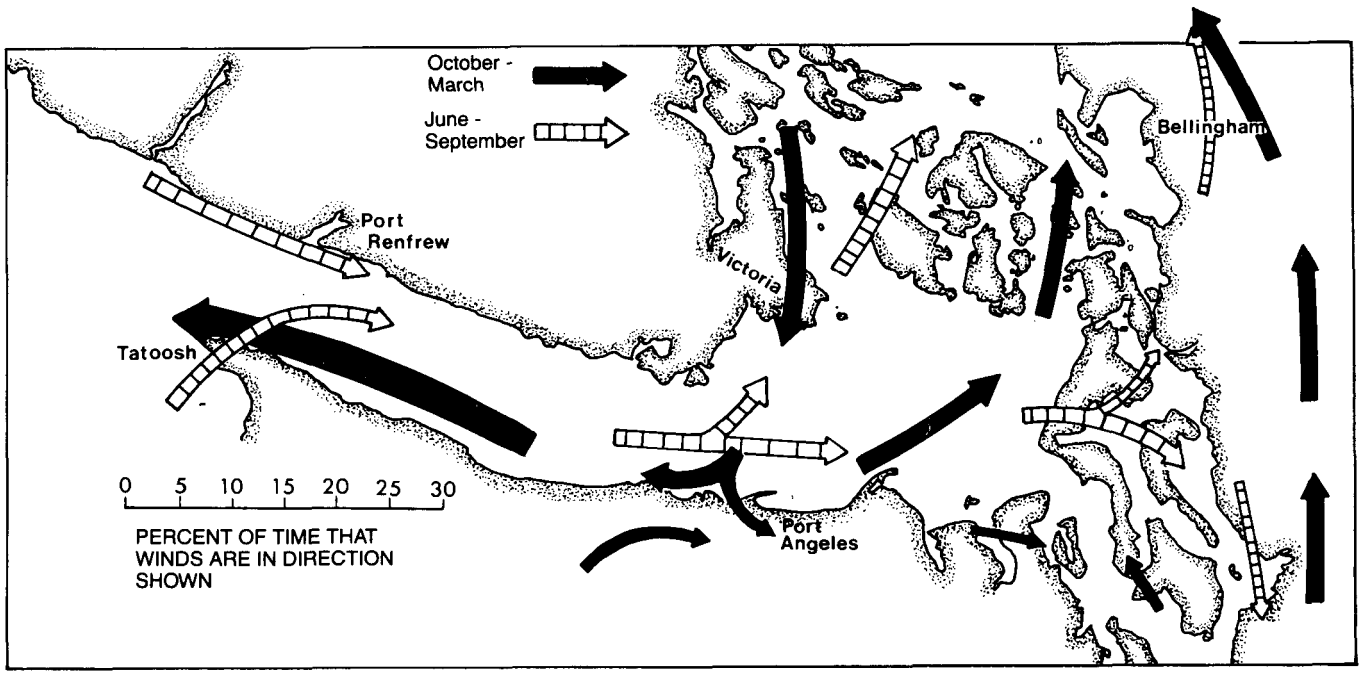

FIG. 11.4. Most frequent pattern of surface winds over Juan de Fuca Strait in winter (solid arrows) and summer (hatched arrows). Thick arrows correspond to wind speeds over 9 m/s (17.5 kn), medium arrows 4.5–9.0 m/s (8.7–17.5 kn), thin arrows less than 4.5 m/s. Comparison of arrow length with scale gives frequency of wind occurrence from given direction. (Compare with Fig. 10.5.) (From Barker 1974)

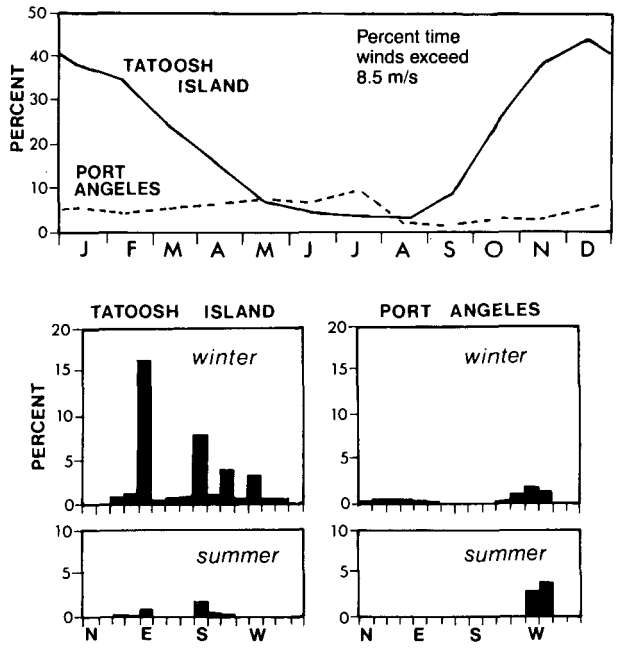

FIG. 11.5. Seasonal distribution of wind speeds greater than 8.5 m/s (16.5 kn) at Tatoosh Island (solid line) off west coast and Port Angeles (broken line). Values in percentages of observations taken 1948–58 for December–February and June–August. (From Holbrook and Halpern 1978)

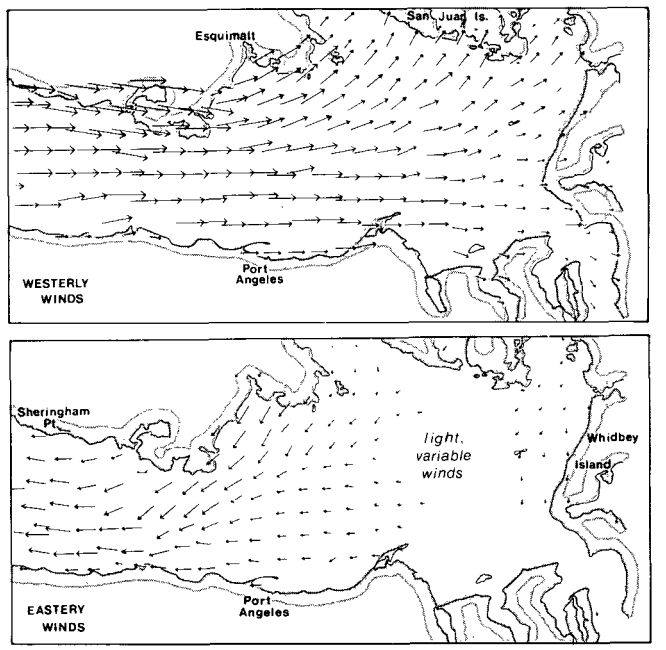

FIG. 11.6. Winds over Juan de Fuca Strait when offshore winds blow from west (*top*) and from east (*bottom*). Wind speeds scaled by relative length of arrows. (From Overland 1978)

they are further enhanced by a strong westerly sea-breeze component. South of Race Rocks the winds branch, part of the air continues eastward into Puget Sound and the remainder blows to the northeast in the direction of the southern Strait of Georgia (Fig. 11.4). Therefore, summer winds at Victoria are predominantly from the southwest at speeds of around 7.5 m/s (15 kn). In fact, from June through August, winds are from the southwest quadrant 80–85% of the time at Victoria and 75% of the time at Port Angeles. Summer winds generally reach maximum

speeds around late afternoon, following near zero speeds in the early morning. The frequency of winds from a given direction in the eastern portion of Juan de Fuca Strait is shown in Table 11.1 for Race Rocks. (Unlike many meteorological shore stations, winds measured there are closely representative of conditions over the water, as are winds measured at Tatoosh Island at the seaward entrance to the Strait. Winds recorded at Ediz Hook at Port Angeles are least representative of winds over the water.)

Two important features of the wind patterns in Juan de Fuca Strait not associated with the large-scale oceanic wind regime are the polar outbreaks in winter and the sea breeze in summer. Known locally as gap winds, polar outbreaks frequently occur under clear skies and near-freezing temperatures that accompany the build-up of a high-pressure region over the interior of Washington State. Driven seaward from high to low pressure, the dense arctic air is accelerated from weak winds at Port Angeles to strong easterly winds at the entrance to the Strait. Arctic air also surges southward at this time to produce northerly winds over the Puget Sound–Seattle area.

During summer, a moderately strong westerly sea breeze builds along the Strait as daytime heating of the land draws cooler marine air inward toward the interior of northwestern Washington and southwestern British Columbia. These winds often augment the westerly oceanic winds to cause an up-channel increase in speed, although the west-to-east difference is typically much less pronounced than the down-channel acceleration of the wind in winter.

As with most areas of rough terrain, Juan de Fuca Strait is a difficult region to predict winds. Mariners who have lost faith in "small craft warnings" issued by Canadian and American weather offices should appreciate that such warnings are based on assumptions about the relationship between air-pressure distributions over the region and corresponding surface winds. But, even if the wind-pressure assumptions were 100% reliable, the weatherman must first predict the pressures before he can predict the winds. And second guessing the rapid evolution of pressure systems along the coast is far from straightforward. It is quite common, for instance, for storm fronts approaching the coast to stall, dissipate offshore, and then move suddenly inland in an unpredictable manner. Perhaps high-speed computers combined with a better understanding of atmospheric dynamics will alleviate many of these problems in the future.

Waves

No direct measurements of waves have been made in Juan de Fuca Strait, so empirical wind–wave relationships are relied on to estimate their height distributions. For easterly winds, the maximum attainable seas will clearly be limited by the total along-the-strait fetch of about 160 km (85 nm), and to a lesser extent by the duration and strength of the wind. The same also applies to seas generated by westerlies in the Strait. In the latter case, the associated offshore winds blow parallel to the outer coast rather than parallel to the axis of the channel, whereby the

TABLE 11.1. Percentage occurrence of winds from a given direction, and mean wind speed regardless of direction, for each month at Race Rocks light station (July 1969 to January 1974).

	MONTH											
	J	F	M	A	M	J	J	A	S	O	N	D
N	24	18	14	8	3	2	2	3	9	15	22	26
NE	27	29	17	11	6	3	3	2	13	21	28	29
E	6	12	10	5	4	2	2	2	7	10	12	10
SE	4	7	7	5	7	4	5	3	8	9	8	7
S	2	3	3	3	2	3	2	3	6	5	3	3
SW	6	5	7	7	9	10	10	11	9	9	5	6
W	29	24	40	59	69	75	76	76	46	28	20	17
NW	2	2	2	2	0	1	0	0	1	2	2	2
Calm	0	0	0	0	0	0	0	0	1	1	0	0
Mean speed (kn)	14.2	10.9	10.6	12.6	13.1	13.4	14.2	13.3	9.3	8.3	10.1	12.2
Mean speed (m/s)	7.3	5.6	5.4	6.5	6.7	6.9	7.3	6.8	4.8	4.3	5.2	6.3

seas they generate rarely progress very far inland before they encounter the shore. Moreover, strong winds along the coast are generally linked to rapidly moving frontal systems of limited duration and extent. Sustained polar outbreaks that blow seaward along the Strait for a day or so, and stationary fronts associated with intense low-pressure cells, presumably produce the largest seas.

Table 6.2 shows that fully developed seas in Juan de Fuca Strait can attain significant wave heights of 1.5 m, or most probable maximum heights of 2.7 m, for a 10 m/s (20 kn) wind that blows for at least 10 h over a fetch of 140 km (75 nm). Under these conditions, only about 10% of the waves would be somewhat higher than 3 m. In general, however, the fetch is typically less than 100 km and fully developed seas would not usually be expected to exceed heights of 2 m. Therefore, if Juan de Fuca Strait wasn't directly exposed to the Pacific Ocean, observed waves would be similar to those in the Strait of Georgia. In reality, of course, swells that propagate inland from the open waters appreciably alter the nature of the observed wave field in the Strait by increasing the overall height of the seas and causing them to steepen. Because the continued existence of swell waves does not require energy input from the wind, the longer waves can penetrate the entire length of the Strait regardless of the winds, and slowly decrease in height as they travel along the channel. Based on wave records off Tofino on the west coast of Vancouver Island, maximum probable wave heights near the Strait entrance can be expected to exceed 6 m at least 10% of the time in winter and 3 m about 10% of the time in summer. The period of this swell ranges from about 6 s to over 20 s, but most commonly lies between 9 and 10 s. Due to dispersion, refraction, and dissipation, the height of the swell will continually diminish inward along the Strait. Even exceptionally large, deep-ocean swell will be reduced to a low ground swell by the time it reaches the eastern portion of the channel.

Rips occur off prominent points and over banks, and are especially heavy off Cape Flattery, Race Rocks, New Dungeness, and Point Wilson at the entrance to Admiralty Inlet. There are dangerous rips at the approaches to Haro Strait, Rosario Strait, and in the area from Trial Island to Discovery Island. River discharge from the San Juan River can produce rips in the vicinity of Port San Juan most of the year.

Tides

The oceanic tide that travels northward along the west coast of North America enters Juan de Fuca Strait as a long, progressive wave whose speed and range vary eastward as a result of changes in the depth and geometry of the channel. For practical purposes such as tidal predictions, hydrographers decompose this wave into various constituents (see Chapter 3) whose individual characteristics can readily be determined through shore-based tide gage observations. In this section, the two main constituents, the semidiurnal wave component (M_2 tide) and the diurnal wave component (K_1 tide), will be used to describe the nature of the "real" or combined tide within the Strait.

It takes about 3.5 h for the M_2 tide to propagate from the Pacific entrance of Juan de Fuca Strait to the vicinity of the San Juan Islands, but only 1.5 h for the K_1 tide to cover the same distance. As a consequence, a particular stage of the incoming oceanic tide occurs roughly 1.5–3.5 h later at the eastern end of the channel. There is a further delay of about 1 h as the tides work their way northward through the narrow passes of the San Juan and Gulf Islands into the southern Strait of Georgia.

As elsewhere on the coast, the combination of a semidiurnal tide and a diurnal tide produces mixed-type tides in the Strait. These have two high and two low waters each day with a distinct diurnal inequality in the heights and times between successive high waters and successive low waters, and a consistently greater inequality in low waters in all regions. Unlike other areas, the shift in balance between the M_2 and K_1 constituents causes a change in character of the tide as it moves inland along the channel (Fig. 11.7). Thus, from the entrance to the vicinity of Race Rocks, the tides are mixed, mainly semidiurnal because the M_2 tide outweighs the K_1 tide. From Race Rocks to the southern Strait of Georgia they become mixed, mainly diurnal as the diurnal (K_1) tide gains in importance. This change in the nature of the tide is directly related to the increasing importance of the moon's declination, which causes the K_1 tide in the first place. In fact, the declinational effect grows so strong near Victoria that the tide becomes diurnal with only one pronounced high and low water each day for about 20 days a month (see Fig. 3.5). This effect decreases northward into the Strait of Georgia and southward into Puget Sound where tides are never diurnal. The interplay between the two main components of the tide also produces a change in the sequence of high and low waters part way along the channel; west of Victoria the sequence is Higher High Water, Lower Low Water, Lower High Water, Higher Low Water; but east and north of Victoria the sequence of tides is Higher High Water, Higher Low Water, Lower High Water, Lower Low Water.

As a consequence of the tide's peculiar nature around Victoria, it is imperative not to use it as a reference when attempting to estimate the tides or tidal streams at other localities; Fulford Harbour is much more reliable. The comparison of tides in Victoria Harbour and those in Oak Bay just a few kilometres around the corner to the north is an example of the complexity. Although Higher High

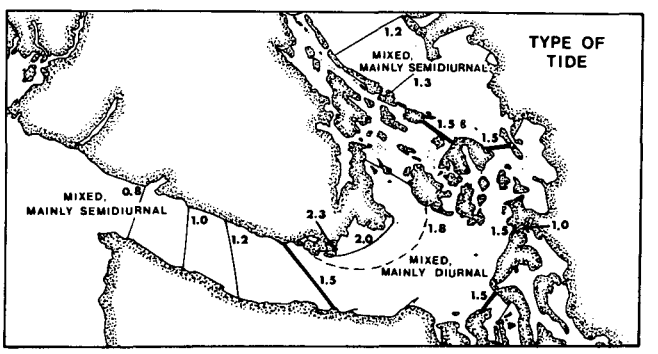

FIG. 11.7. Chart shows change in type of tide along Juan de Fuca Strait. Lines give values of ratio of diurnal tides to semidiurnal tides $(K_1 + O_1)/(M_2 + S_2)$. (See Chapter 3 for further details.) (From Parker 1977)

Water is normally about the same at these two places (2.5 m at Victoria compared to 2.6 m, at Oak Bay) the time of the tide is 58 min later at Oak Bay. Similarly, Lower Low Water is 0.7 m at both locations, but is delayed 22 min longer at Oak Bay.

The decrease in relative importance of the semidiurnal tide along Juan de Fuca Strait is shown in Fig. 11.8a, where its range is plotted as a function of distance. Because the opposing up-channel increase in the range of the diurnal tide (Fig. 11.8b) is not enough to counterbalance this effect, the overall range of the tide also exhibits an eastward decrease toward Victoria. Mean tidal ranges in Fig. 11.9 diminish from 2.4 m off Cape Flattery to a minimum of 1.8 m near Victoria, then increase again to around 2.4 m at the northern end of Haro Strait. A further indication of the complexity of tides near Victoria is the fact that the semidiurnal part of the tide attains its minimum range at Pedder Bay; on the other hand, the diurnal portion of the tide attains its maximum range at this location. Pedder Bay, it seems, is located at a distance from the northern end of the Strait of Georgia where the surviving remnant of one reflected tidal wave that propagates toward the ocean (see Chapter 3, 10) has its maximum cancelling effect on the next tidal wave that propagates inward from the ocean.

The considerable effect of the rightward turning Coriolis force is clearly displayed by the tidal range which, for the K_1, M_2, and total tide, has a marked increase across the Strait from the Canadian to American sides. In the case of the M_2 tide, for instance, the range at Pedder Bay is about 0.7 m; on the directly opposite side of the Strait at Port Angeles the tidal range is 1.0 m. Moreover, there is a tendency of the tide to occur a few minutes earlier on the American side as the tide leans to the righthand side of the channel on its way toward the Strait of Georgia.

Lastly, of course, the tidal range in Juan de Fuca Strait undergoes a biweekly variation due to shifts in the declination of the moon, to changes in the alignment of the sun and moon, and to alteration of the moon's distance from earth. These, together with other periodic changes in the tidal range, were discussed in Chapter 3.

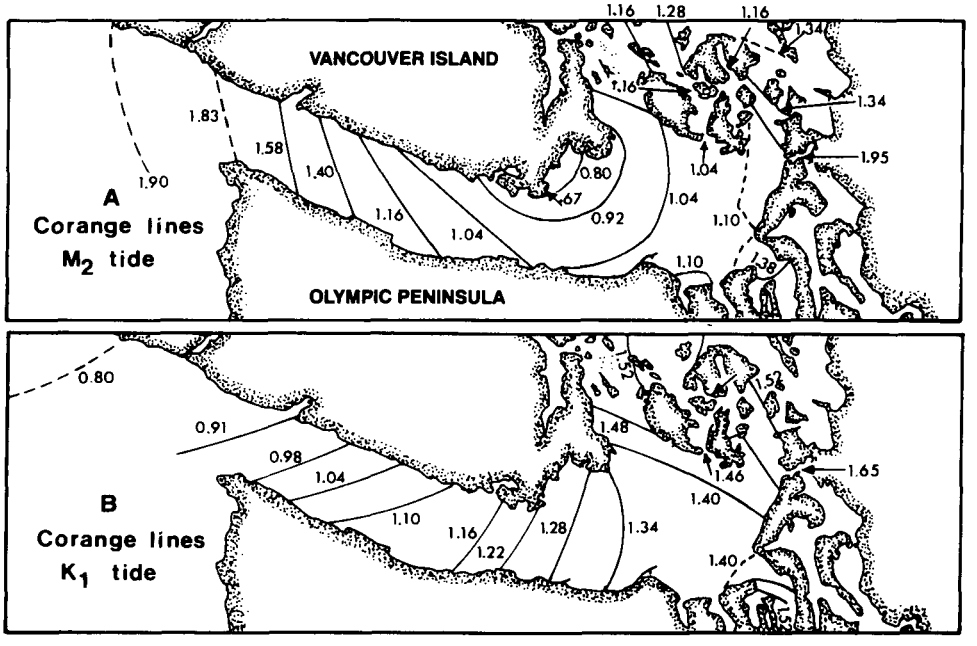

FIG. 11.8. Corange lines (m) in Juan de Fuca Strait. (A) Major semidiurnal constituent, (B) major diurnal constituent. (From Parker 1977)

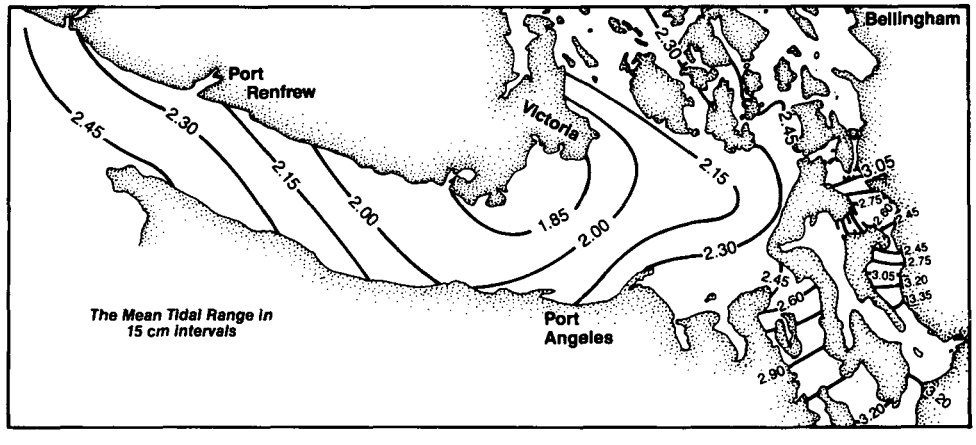

FIG. 11.9. Mean tidal range in Juan de Fuca Strait (m). (From Barker 1974)

Tidal Currents

Major factors that affect currents in Juan de Fuca Strait are tides, freshwater runoff, winds, and along-channel atmospheric pressure differences. The Coriolis force, channel curvature, and bathymetry modify the currents once they become established. Although the relative importance of these factors varies over the length and breadth of the Strait, the combination of a uniform geometry, a fairly regular shoreline, and the lack of direct river discharge tends to produce a comparatively straightforward flow structure. This is certainly true relative to the complex current regimes in the Strait of Georgia. However, Juan de Fuca Strait is not without its own idiosyncrasies. The oceanography of the western sector of the Strait, for example, is influenced strongly by wind and current events along the outer coast; in the eastern sector, "normal" flow patterns are regularly disrupted by strong tidal streams that emanate from connecting channels that open into the main basin. Therefore, what follows is at best a generalization of the flow structure in the Strait, beginning with the tidal streams generated by the oceanic tide.

The tide within Juan de Fuca Strait has the nature of a progressive-type wave that has been measurably modified by the presence of a standing wave component. For a pure progressive tide, flood streams at a particular location are strongest near the time of local high water and ebb streams strongest near the time of local low water. The greater the contribution from a standing wave component, the longer the time of maximum flow lags behind the time of extreme high (or low) water. Therefore, because of the along-channel variation in the importance of the standing wave, the correspondence between the tide height and the tidal streams varies with distance along Juan de Fuca Strait. Near the Pacific entrance, the appreciable standing wave component causes the current (for instance, maximum flood) to lag behind the tide (local high water) by 1–1½ h. In the area between Race Rocks and Angeles Point, however, there is only a small time lag between the tide and the tidal streams, because the tidal wave within the eastern part of the Strait has the nature of a nearly pure progressive wave. East of this region, the roles reverse and the tide lags behind the current as the tidal propagation again begins to depart from that of a progressive wave. This lag increases steadily as far as the Strait of Georgia, where maximum flood streams always precede high water by about 3 h and maximum ebb streams always precede low water by 3 h. The natural sequence of currents in Juan de Fuca Strait always follows the same general pattern of stronger maximum flood, weaker maximum ebb, weaker maximum flood, and stronger maximum ebb (Fig. 11.10).

Flood streams are northward along the Washington coast and turn into Juan de Fuca Strait north of Cape Flattery (Fig. 11.11). In this area, they initially set toward the Vancouver Island shore but further inland they are directed down-channel by the confining geometry of the basin. By maximum flood, the water moves parallel to the axis of the Strait at all locations at speeds of 75–130 cm/s (1.5–2.5 kn) on large spring tides;speeds of 180 cm/s (3.5 kn) can occur on large tides in the eastern portion of the Strait near the approaches to the major channels. Flood currents are generally a little stronger on the U.S. side of the western channel, due in part to the right-turning Coriolis effect. This difference is small, however, and the mariner should not expect to gain any advantage from it. Only when the currents are averaged over many days or weeks, does the influence of the Coriolis force become apparent.

In the vicinity of Race Rocks and Discovery Island off Victoria, flood currents can at times be accelerated to speeds of around 250 cm/s (5 kn) as they are squeezed through narrow channels. Similar conditions prevail at the entrance to Admiralty Inlet and Deception Pass. As in any passage of this type, dangerous rips can form if the currents oppose the propagation of wind waves or ship waves into the area. At Race Rocks, rips will form on the flood if winds are from the northeast or southeast quadrants, a common situation during winter when winds are from these directions 65–80% of the time. Similarly, rips will occur in the vicinity of Discovery and Trial islands when the winds are from the northeast quadrant on the

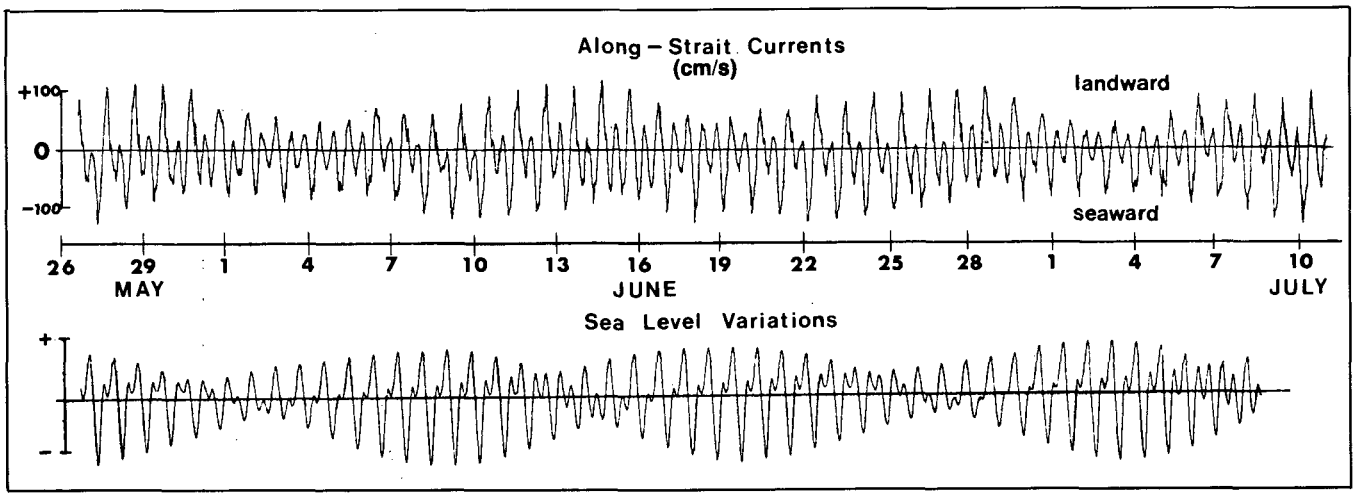

FIG. 11.10. Comparison of ebb–flood sequence and tide height variation in Juan de Fuca Strait. Time in days increases from left to right; currents, cm/s (100 cm/s ~ 2 kn). (Adapted from Fissel and Huggett 1976)

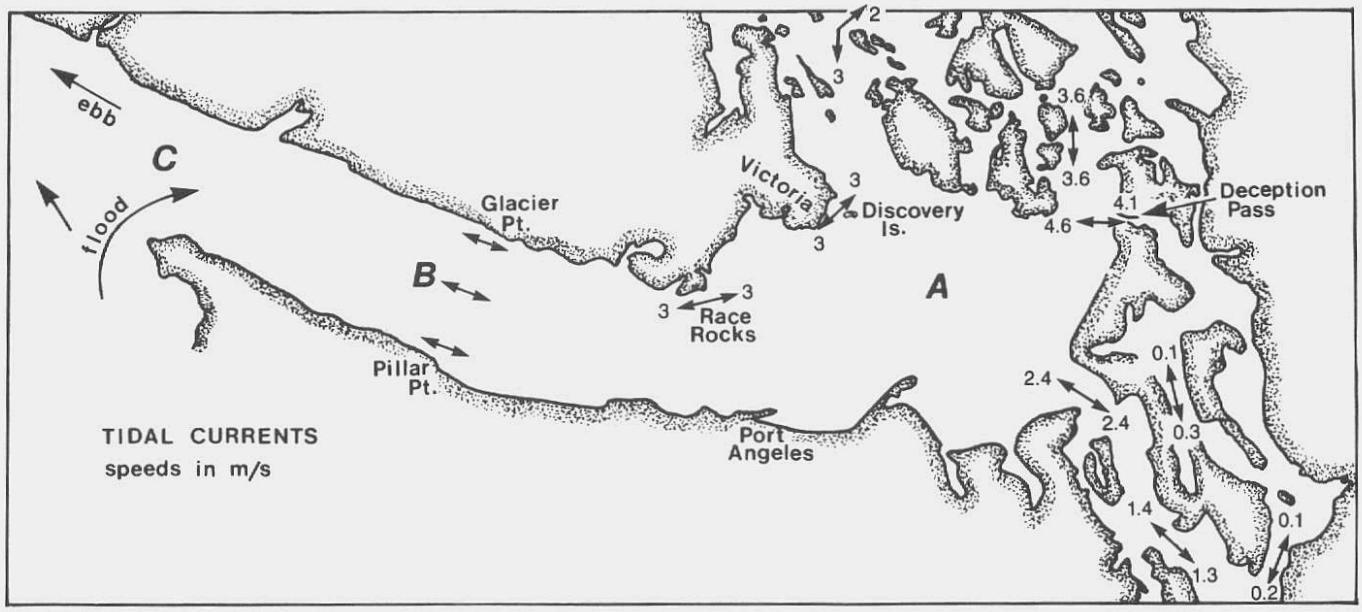

FIG. 11.11. Maximum tidal streams in Juan de Fuca Strait and adjacent passages (1 m/s ~ 2 kn). (A) Maximum ebbs 1.8 m/s, floods 1.5 m/s; (B) maximum streams 1.3 m/s; (C) 0.75 m/s.

flood. In practice, rips will occur anywhere in the Strait where tidal currents are accelerated, such as over banks, shoals, and off prominent points. Because of steep waves, such rips can be dangerous to small boats.

Within the wider eastern section of the Strait, the major portion of the flood sets to the northwest, following the trend of the deeper channels that lead into the Strait of Georgia. Haro Strait accommodates the largest volume of water that moves northward into the Strait of Georgia, followed in turn by Rosario Strait and Middle Channel, while the remainder moves through Admiralty Inlet into Puget Sound. Approximate calculations show that, of the water from Juan de Fuca Strait, 50% goes through Haro Strait, 20% through Rosario Strait, 5% through Middle Channel, and 25% through Admiralty Inlet into Puget Sound. Typical maximum tidal currents for the various passages within, and leading into, Juan de Fuca Strait are shown in Fig. 11.11.

Maximum ebb currents generally flow in the opposite direction to maximum flood currents. Moreover, the change from flood to ebb (and vice versa) at a particular location in the Strait is nearly along a straight line. Without exception, tidal ellipses are flattened and the currents closely rectilinear. Within the narrower portion of the Strait, ebb currents are slightly stronger and of longer duration on the Canadian side than the U.S. side. Near the coastal entrance, tidal currents on the northern side maintain their westerly direction as far as Cape Beale before they merge with the southwesterly setting ebb currents off the B.C. coast. On the Washington side, the streams quickly become part of the southerly tidal flow off Cape Flattery.

As with most channels along the coast, the strength and duration of the tidal streams in the Strait are usually distorted by estuarine-type processes. Consequently, ebb currents are noticeably stronger and of longer duration than flood currents in the top 100 m (Fig. 11.12). Below

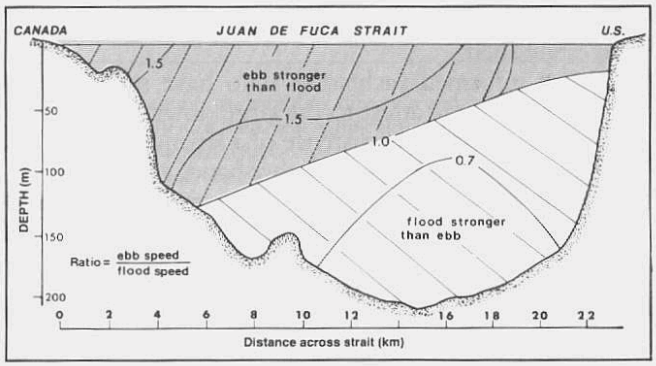

FIG. 11.12. Average ratio of the ebb speed to the flood speed in cross-section from Pillar Point (USA) to Port Renfrew (Canada).

this depth on the other hand, flood currents are normally stronger and of longer duration than ebb currents. This bias toward the ebb in the upper layer is because river runoff into the Strait of Georgia and Puget Sound slowly works its way to the Pacific via Juan de Fuca Strait. By mixing with oceanic water in the passes, the runoff forms a comparatively light surface layer whose general drift seaward somewhat retards the surface flood streams and stengthens the surface ebb streams. Floods are stronger than ebbs below this top layer as oceanic water must drift inward at depth to replace the salt water entrained and carried to the Pacific Ocean within the surface layer.

The "coarse grid" computer model outlined in the previous Chapter gives an overall picture of the depth-averaged tidal streams throughout the main channel of Juan de Fuca Strait. These currents are shown in Fig. 10.14a, b for two stages of a semidiurnal tide. The "fine grid" model provides more detailed information on the flow in the vicinity of the Gulf and San Juan islands. Complete current vector plots for the fine grid are in Fig. 10.15a–c for three stages of the tide.

It is important to remember that these charts do not take into account the presence of the weaker estuarine circulation just discussed. Also, for modeling purposes at the seaward entrance to the Strait, it is necessary to assume that the tidal streams flow parallel to mid-channel, which in reality is not strictly true. A short distance up-channel, the modeled flow should closely resemble actual tidal streams.

A number of especially salient features of the currents are revealed by the computer simulation:

1) During the larger of the two daily floods within Juan de Fuca Strait, a well-defined, counterclockwise backeddy develops to the east of the Race Rocks shoal region. For this to occur, maximum flood streams must attain speeds of around 100 cm/s or more in mid-Strait. Although the details of this flow near Race Rocks are severely limited by the 2-km resolution of the model, it would appear an intense countercurrent is set up, which flows *westward* in the vicinity of Race Passage toward the end of the flood. Moreover, the backeddy continues to expand, while maintaining its strength, until the ensuing ebb. At the time of high-water slack in most of the Strait, the backeddy becomes a strong cross-channel jet that extends a few kilometres from Race Rocks; this disappears once the ebb has been established.

Most informed yachtsmen who have sailed in the Victoria region will attest to the large downstream backeddy on the flood. The existence of a strong counterflow through Race Passage, on the other hand, remains uncertain, although it may account for the apparently anomalous currents Swiftsure racers often encounter in this region.

2) Contrary to the above situation, no backeddy develops east of Race Rocks on the weaker of the two daily floods with maximum flood speeds of around 50 cm/s or less in mid-channel.

3) A strong counterclockwise rotating backeddy develops downstream of Discovery Island on the larger floods (Fig. 11.13); a less intense clockwise eddy forms behind Dungeness Spit on the flood.

4) The turn to ebb begins about 1 h earlier on the U.S. side of Juan de Fuca Strait and comparatively strong currents surge seaward from Admiralty Inlet at the time of high-water slack in the rest of the Strait. At this time, a weak flow extends from Haro Strait across-channel to Port Angeles, where it joins the intensifying ebb along the Washington shore.

5) Flood streams in Haro Strait are strong but confused, especially at the southern approach. Maximum flood speeds are along the western side of San Juan Island and there is a sharp fall-off in speed toward mid-channel; on the Cordova Bay side of the Strait, currents are relatively weak and irregular. Observations in Haro Strait verify the presence of much stronger flood streams along the San Juan Island side of the channel.

6) The flood streams in Rosario Strait split around Cypress Island with nearly equal speeds on either side, but tend to reunite south of Sinclair Island. Tidal streams within Bellingham, Samish, and Padilla bays are always weak despite the large tidal range.

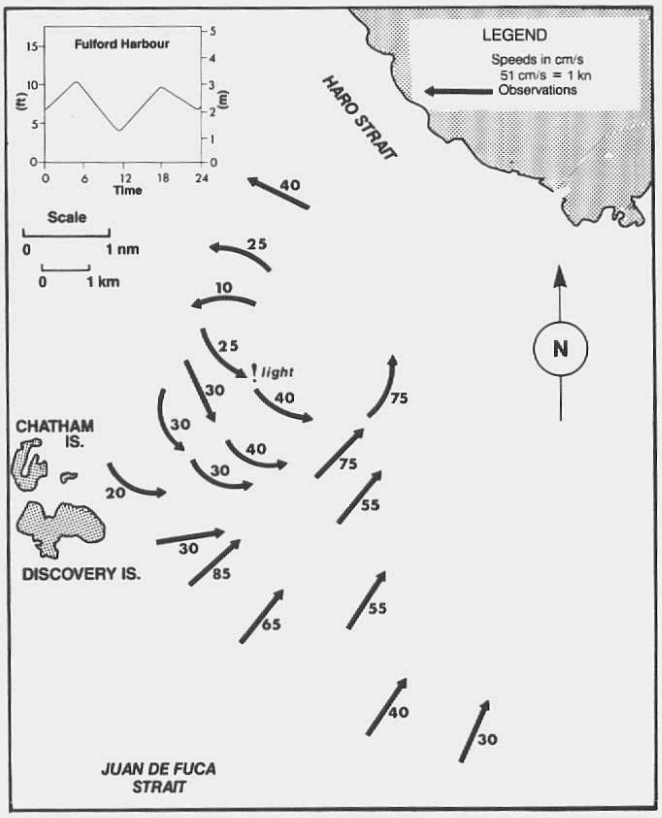

FIG. 11.13. Observed surface flood currents at southern approach Haro Strait. Speeds based on aircraft tracked surface drifters. (Courtesy S. Huggett and P. Crean)

7) After the flood stream rounds the corner at East Point in Haro Strait, it divides, with strong flows in both President Channel and Boundary Passage. These flows then reunite at the Strait of Georgia end of Boundary Passage to produce a jetlike flow that veers to the north in the Strait. At this time, a large counterclockwise backeddy is established north of Saturna and Tumbo islands. As with backeddies in Juan de Fuca Strait, this eddy expands throughout the flood and persists until the ebb has begun. Maximum speeds are off the north shore of those islands and directed to the east.

8) During the ebb, tidal streams in Juan de Fuca Strait are directed seaward everywhere along the channel and no large backeddies are formed, according to the model results. However, there would appear to be a rather weak clockwise backeddy in the lee of Discovery Island.

9) During moderate ebb conditions, there is apparently a weak nearshore countercurrent along the western side of San Juan Island until about maximum ebb. Midway through the ebb this current reverses and joins the normal seaward flow through Haro Strait.

Observed Currents

The computer model of the time-varying currents in Juan de Fuca Strait considers only the contribution from tidal streams generated by tidal forces of the moon and sun. Consequently, actual currents may deviate somewhat from the model results because of the smaller, but far from

negligible, contributions by the estuarine current regime, density currents, and wind currents. Eventually, these effects, too, will be included in future models, but until then only direct measurements give a full understanding of the strength and variability of the total flow.

Direct measurements of currents in Juan de Fuca Strait over the last decade by Canadian and American scientists reveal the flow is essentially parallel to the trend of the channel at all stages of the tide. Slight deviations from these directions are possibly due to remnant intrusive motions originating with strong currents from the major tidal passages or to the deflecting influence of points of land, for instance off the coast between Slip point and Pillar Point on the Washington side and east of Otter Point on the British Columbia side (Fig. 11.14).

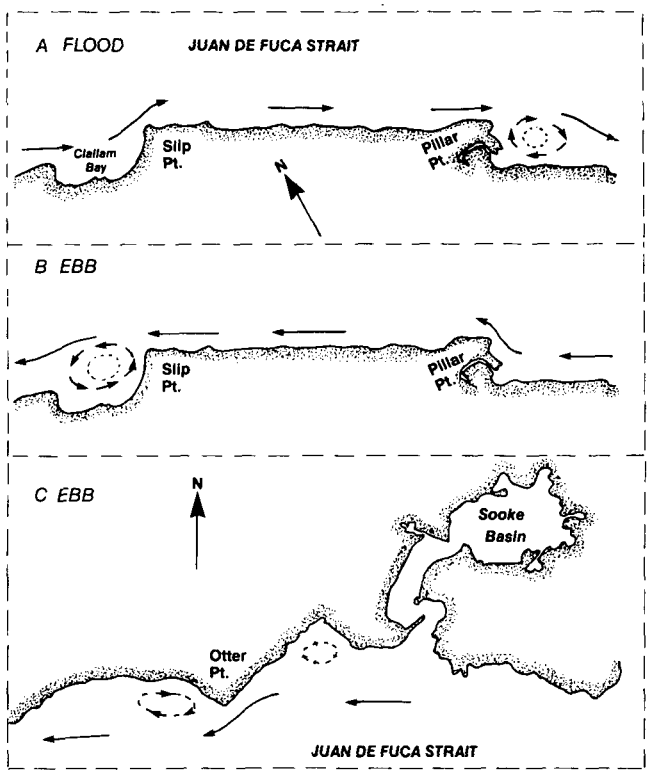

FIG. 11.14. Formation of backeddies in Juan de Fuca Strait. (A) flood, (B) ebb, along southern shore, central Strait, (C) ebb along northern shore, eastern Strait.

Within the broad eastern portion of the Strait, currents are typically east–west, but swing more to a north–south orientation near the approaches to the major channels that lead to the Strait. Due to the confined nature of Juan de Fuca Strait, moreover, the currents tend to be rectilinear (see Chapter 3), whereby the direction of the flood and ebb are diametrically opposite with very little rotary turning. Nevertheless, in mid-channel and off the Pacific entrance, the current vectors have a tendency to rotate clockwise during a tidal cycle to form a somewhat flattened ellipse (Fig. 11.15). The rotary behavior is slightly more developed in the broader, eastern portion of the Strait.

The estuarine circulation (a net seaward flow of rela-

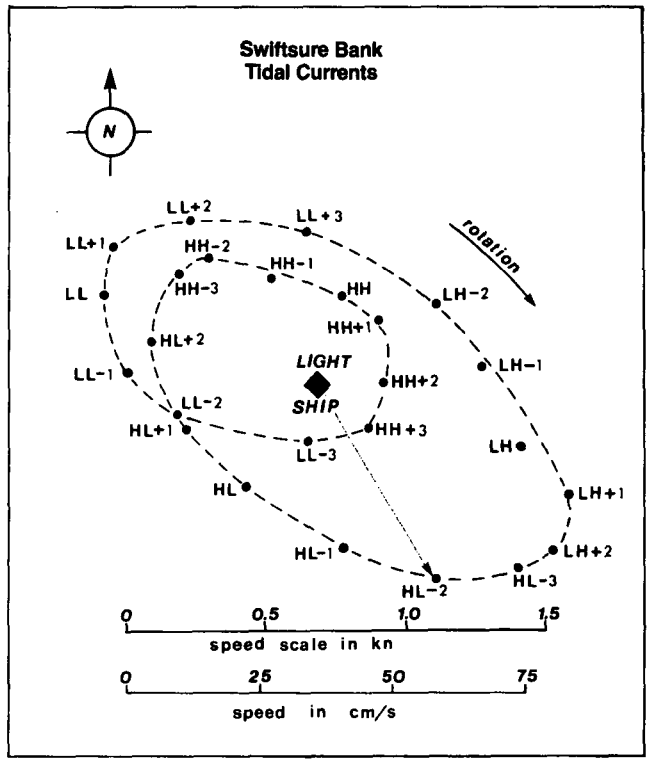

FIG. 11.15. Diagram to determine direction and speed of rotary tidal currents over Swiftsure Bank near Tropic tides (maximum lunar declination). To determine tidal current for particular time look up state of tide at Tofino, B.C., then draw arrow from Light Ship to appropriate time position on dashed curve (e.g. HH–1 means time of Higher High Water less 1 h; LH + 2 Lower High Water plus 2 h, etc.) Orientation of arrow gives direction of current flow, length of arrow its speed as determined from scales. Example shows flow to southeast at 42.6 cm/s at 2 h after Higher Low Water. (Adapted from Marmer 1926)

tively low-density water in the upper 100 m of the Strait with a compensating inward flow of more dense water at depth) becomes apparent when the tidal streams are subtracted from the current meter records. Near the surface, this residual flow has typical seaward speeds of 10–20 cm/s (0.2–0.4 kn), becomes as great as 40 cm/s (0.8 kn) in early summer, with maximum values concentrated close to mid-channel in the western portion of the Strait. East-setting residual flow within the lower layer is around 10 cm/s and strongest away from mid-channel (Fig. 11.12). The across-strait tilt of the line separates net seaward flow in the upper layer from net landward flow in the lower layer (Fig. 11.12) and is due to the combined effects of the Coriolis force and channel curvature. In this case, the outflow favors the Canadian side, whereas the inflow favors the American side.

If the residual currents in Juan de Fuca Strait were steady, or at worst variable in some predictable fashion, very accurate predictions of currents could be obtained by computer simulation models. Unfortunately, there are significant variations in this flow both with time and location due to poorly understood changes in the estuarine processes that produce it. Thus, even though the residual current in the surface layer of the Strait moves seaward on average, it is sometimes observed to "stall" for several days at a time and on occasion reverse direction

completely. On a seasonal basis, reversals in the near-surface residual current are least likely in summer, when the driving mechanism for the flow (freshwater discharge into the inshore waters) is at its maximal strength. Prevailing northwest winds at this time also tend to favor a strong, persistent seaward flow. Within the Strait of Georgia, these winds help move the brackish Fraser River runoff into Juan de Fuca Strait, whereas off the coast they drive oceanic surface waters away from the mouth of the Strait, lower sea level, and increase the east–west hydraulic head along the channel.

During fall and winter, the above processes are modified considerably and landward residual currents frequently occur in the near-surface waters with an accompanying seaward residual flow at depth. River discharge is minimal at this time and southerly winds prevail over the coast. Not only do these winds oppose the movement of brackish water into the eastern end of Juan de Fuca Strait but they also tend to raise sea level at the seaward end, which counters the normal east–west hydraulic head associated with the outflow of fresh water. Recent observations indicate that time-averaged, near-surface currents may flow up-channel in winter for 3–10 days, extend as far as Race Rocks 90 km inland, and attain speeds in excess of 50 cm/s (1 kn) for a day or so (Fig. 11.16A). At such times, ebb currents would be weak whereas flood currents would be anomalously strong. Present indications are that such eastward directed residual flows are directly linked to slow (25 km/day) eastward propagation in the Strait of a long internal bore. Generation of this wave is, in turn, apparently linked to southerly storm winds along the outer Washington coast. Figure 11.16B provides further evidence for reversals in surface flow in the Strait during offshore southwesterlies. In this case, warmer oceanic surface water was driven over 100 km along the southern half of the channel before being carried seaward following break-down of the offshore wind system. One thing is certain, no one should expect currents in Juan de Fuca Strait to behave at all times as predicted in the tide tables.

To close this section, a few additional remarks can be made regarding currents in Juan de Fuca Strait.

1) Current predictions for Race Rocks in *Canadian Tide and Current Tables*, Vol. 5 are based on observations taken about 4.5 km south of Race Rocks and not on measurements within Race Passage. Furthermore, the predictions attempt to take into account the residual flow contribution to the ebb and flood speeds, which may possess considerable day to day variability.

2) The times of the turns and maximum tidal streams at locations between Jordan River and Pillar Point on the U.S. side occur 30 min earlier, on the average, than those south of Race Rocks. Variations from this average are at most 30 min but occur irregularly from one tide to the next. Thus, for example, maximum tidal currents half way between Pillar Point and Jordan River may occur between zero and 60 min earlier than at Race Rocks.

3) Current predictions for Juan de Fuca Strait in *Canadian Tide and Current Tables* are based on measurements made in mid-channel near the seaward end early this century and, therefore, should be used with cautious optimism about their accuracy. Variations in the strength and direction of the surface residual flow, together with variable ocean current regimes off the coast, can lead to marked departures of the predictions from actual currents. A comparison of the Race Rocks and Juan de Fuca Strait predictions indicates that times of the turns and maximum tidal streams at the Strait entrance lead those at the eastern

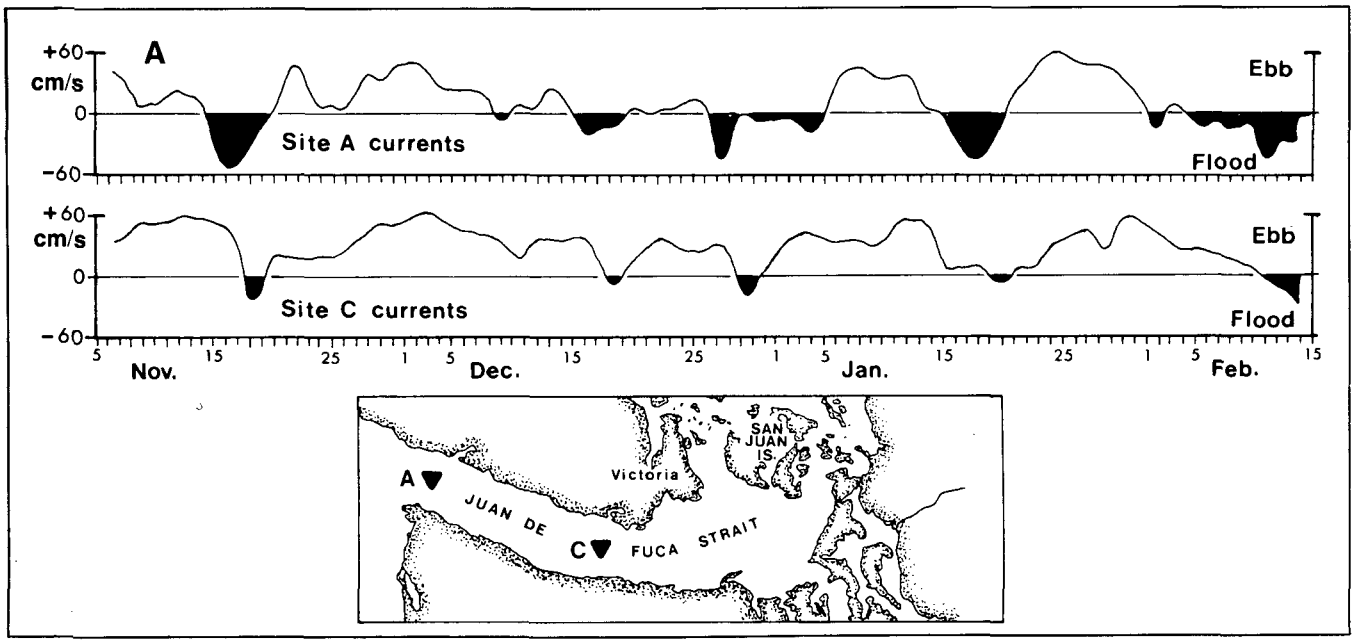

FIG. 11.16. (A) Variation in speed and direction of nontidal, along-channel surface currents in Juan de Fuca Strait. Currents (cm/s) measured at depths of 4 m at A and C from November 1976 to February 1977. Up-channel (flood direction) reversals in mean flow at seaward approach are often few days later at Site C, 60 km inland. (Adapted from Holbrook and Halpern 1978).

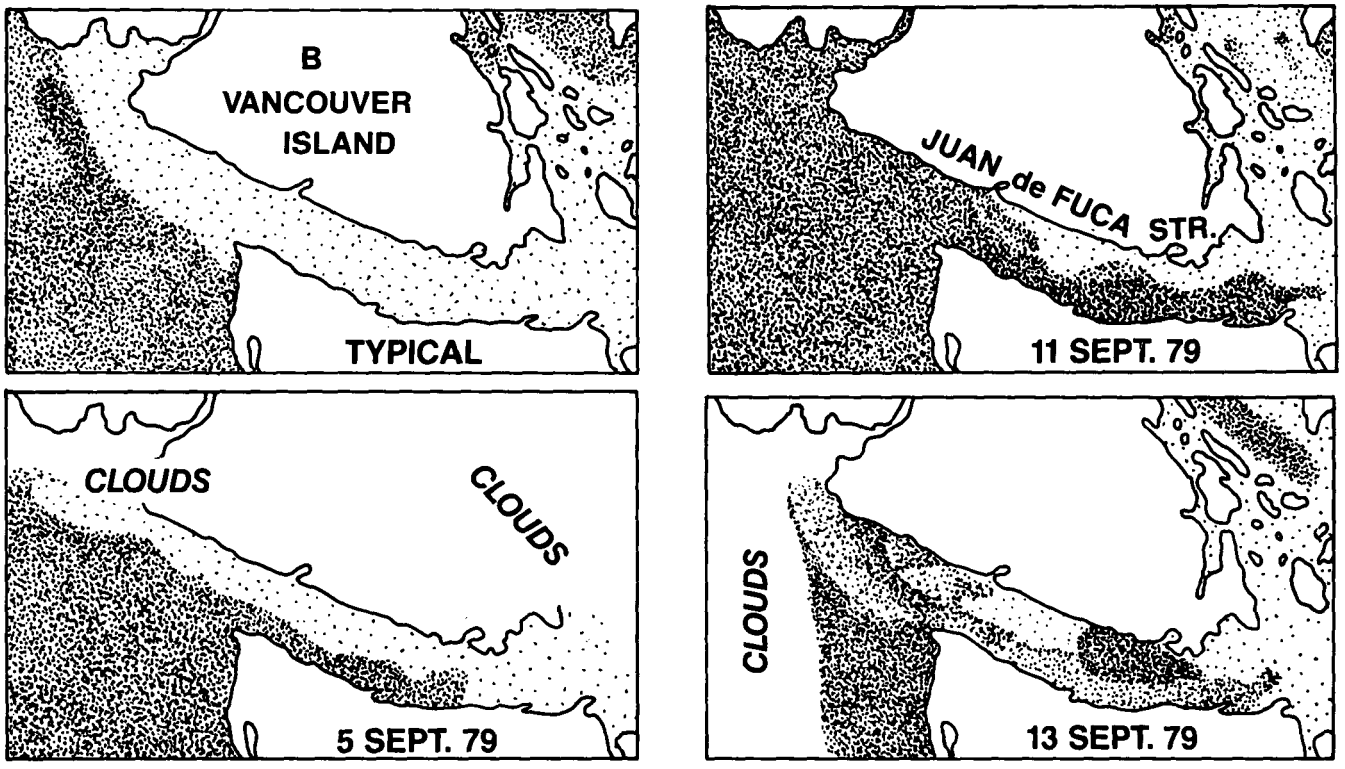

FIG. 11.16. (B) Drawings based on infrared satellite images of sea-surface temperatures, showing sequence of warm-water intrusion (heavy stippling) into Juan de Fuca Strait from the Pacific Ocean in September 1979. Offshore coastal winds were from the southwest and associated with a low-pressure system off the coast. Intrusion was confined mainly to the southern half of the Strait and reached a maximum of 135 km from the entrance. Four days after cessation of the southwest winds, the seaward estuarine circulation was reestablished and the intrusion began to be advected out of the Strait. (Courtesy, J. Holbrook)

end of the channel by 1–1½ h, on the average. The major exception is at the turn of the weaker of the two daily floods that are predicted almost simultaneously along the Strait.

4) Tidal currents over banks and shoals away from the shoreline will generally be stronger than those in adjacent deeper waters. However, due to frictional effects, nearshore tidal streams will be weaker than those in mid-channel and turn to ebb or flood ½ h or so earlier.

5) Nearshore currents downstream of a point of land will form backeddies if there is an accompanying increase in the width of the channel; this occurs to the east of Pillar Point and Race Rocks on larger floods. Nearshore currents will be deflected toward mid-channel as they approach a sudden decrease in channel width as when the ebb approaches Pillar Point from the east. Both deflections and backeddies will be associated with symmetric points like Otter Point near Sooke (Fig. 11.14).

6) Tidal currents in the vicinity of Swiftsure Bank seaward of the entrance to the Strait are strongly rotary, change direction in the clockwise sense about every 12½ h, but only slightly alter their speed as they change direction (Fig. 11.15). Maximum floods are southeast at about 75 cm/s (1.5 kn) and maximum ebbs northwest at around the same rate.

7) Nontidal currents over Swiftsure Bank are primarily the result of coastal wind systems and are predominantly northward in winter and southward in summer. The surface wind currents attain maximum speeds of roughly 100 cm/s (2 kn) with minimum speeds of 25 cm/s. These currents join with the tidal currents to produce a complicated anticlockwise circulation off the entrance to the Strait with westward currents to the north, eastward currents to the south, and a northerly cross-channel current setting toward Vancouver Island from the vicinity of Cape Flattery.

Sooke Inlet

Sooke Inlet is the second of two major bodies of water that open into Juan de Fuca Strait on the Vancouver Island side. Named after the Soke Tribe, which was all but wiped out by a confederation of other local indian tribes around 1848, the inlet actually consists of three main sections (Fig. 11.17): Sooke Basin, the deepest portion with a length of approximately 3 km, a mean depth of 17 m, and greatest depths of about 30 m near its seaward end; Sooke Harbour, basically a 3-km long sill between Billings and Whiffin spits, with an average depth of only 3 m; and Sooke Inlet proper, a short channel that connects the area to the Strait.

The mean tidal range within the inlet is around 2.0 m but reaches 3.2 m on large tides. Freshwater inflow into the area is mostly from the Sooke River which, like other rivers on Vancouver Island, attains maximum discharge in winter and has little runoff in summer. (It is during this

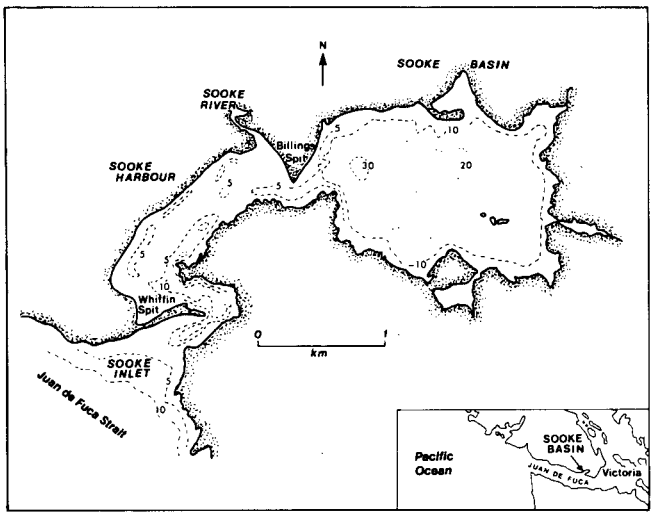

FIG. 11.17. Map of Sooke Basin and adjoining waters. Depths in metres.

low runoff period that the "Sooke Potholes" in Sooke Hills watershed offer some of the most pleasant swimming for residents of the area.)

Water properties throughout Sooke Inlet are largely determined by the combined influence of tidal exchange with Juan de Fuca Strait and freshwater input via the Sooke River. During the winter, salinities are lowest due to river discharge, typically around 20‰ at the suface with a gradual increase to values of 31‰ near the bottom in Sooke Basin as a result of saltwater penetration from the Strait. Water temperatures at this time are comparable to those in the Strait, a chilly 7–10°C, throughout the entire depth of the inlet (Fig. 11.18a). From March onward the water properties begin to change as the river outflow diminishes. This change is marked by a tendency to uniformly high salinities (31–31‰) throughout the entire inlet in summer and an increase in temperatures as solar heat is retained in the upper layer. By August (Fig. 11.18b), the upper few metres of the eastward end of Sooke Basin may be as warm as 20°C depending on weather and wind conditions. Due to tidal mixing, such comfortably warm water will be limited to the Basin; along Sooke Harbour and Sooke Inlet proper there is a marked decrease in temperature toward the ever-cold waters of Juan de Fuca Strait.

The few current observations available for Sooke Inlet show that maximum ebb–flood streams occur off Whiffin and Billings spits in Sooke Harbour, with appreciably lower speeds in other portions of the inlet. Maximum streams are set up roughly midway through a tidal cycle and slack waters are near the times of low and high tide at Sooke. Flood streams along the axis of the inlet during a rise to large high tide can attain speeds of 100 cm/s (2 kn) off Whiffin Spit and 150 cm/s (3 kn) off Billings Spit. Ebb streams during a fall to large low tide, on the other hand, are somewhat weaker because of frictional effects, and attain maximum speeds of approximately 50 cm/s off both prominences. During mean tides, the corresponding speeds for both the ebb and flood are reduced by about a factor of 3. Within Sooke Harbour away from the approaches to the spits, and at the seaward entrance to the inlet, maximum tidal streams are typically less than 15 cm/s, and rise at most to 50 cm/s (1 kn) during large tides.

Tidal streams within Sooke Basin are always weak (less than 20 cm/s; 0.4 kn) and appear to form a clockwise gyre centered over the deeper western portion (Fig. 11.19) due to the fact that the flood keeps mainly to the north side of the basin while the ebb prefers the south side. The confined nature of the weak circulation makes the basin a favorable oyster cultivation region, and accounts for about 25% of British Columbia's commercial oyster production.

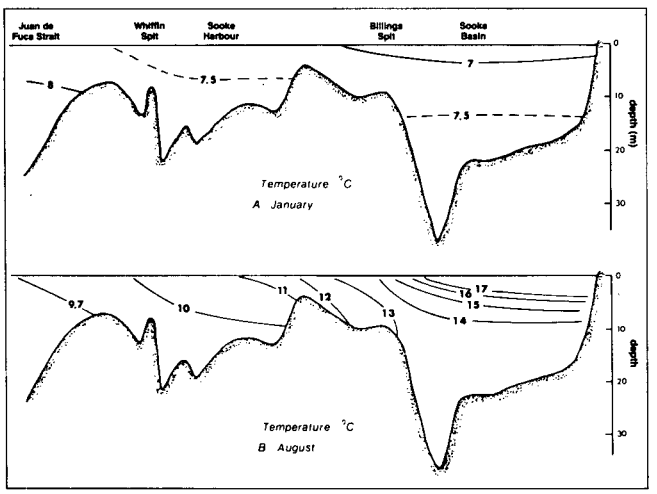

FIG. 11.18. Temperature distribution along mid-channel from Juan de Fuca Strait to head of Sooke Basin (A) January 1966, (B) August 1966. (From Elliott 1969)

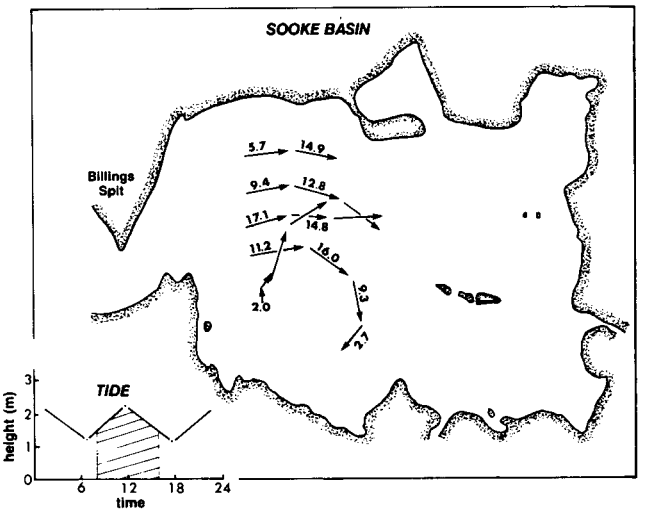

FIG. 11.19. Trajectories of drogues in western sector of Sooke Basin at 2 m, with estimated currents (cm/s). Hatched area lower left shows tide height during time drogues were tracked. (From Elliott 1969)